



AN EXPERIMENTAL APPROACH FOR INTAKE MANIFOLD TUNING FOR INTERNAL COMBUSTION ENGINES.

Marcelo Renato Cavaglieri

Thomas Maciel Moura

Magenti Marelli Powertrain Brazil, Av. da Emancipação, 801 – Hortolândia – SP – Brasil.

e-mails: marcelo.cavaglieri@magnetimarelli.com, thomas.moura@magnetimarelli.com

Prof. Dr. Rogério Gonçalves do Santos

FEM – UNICAMP, Rua Mendeleev, 200 – Campinas – SP – Brasil.

e-mail: roger7@fem.unicamp.com.br

Abstract. *Like it is known, the intake manifold plays an essential task on an internal combustion engine's volumetric efficiency and this significant function has made emerge countless new technologies to improve the air supply through it. Like Variable Length Intake Manifold for example, among others that are able to contribute with a better efficiency using the dynamic effect which happen inside an intake manifold. So, this paper shows an experimental bench able to characterize intake manifolds under its dynamic flow influence on the engine admission process. Supplying so, a support to validate numerical models in optimization process or eliminate expensive and lengthy tests on vehicles. The dynamic admission is similar to the acoustic wave phenomena and its efficiency can be measured using a well known parameter called Transmission Loss, which is no more than the power transfer coefficient. This work shows in details the experimental approach, the function of each component, techniques for Transmission Loss determination and its calibration using classic analytical models to that. Ultimately, it shows a Transmission loss determination for two real Intake Manifolds and the correlated effect when applying both in the same engine model.*

Keywords: *intake manifold, acoustic response, tuning, transmission loss, engine.*

1. INTRODUCTION

As can be seen in Winterbone and Pearson (1999 and 2000) in a regular internal combustion engine (ICE) in the air intake phase, the period when the intake valve is open, it is noted that the cylinder volume is not filled completely, as one wishes theoretically. This is due to the variation in density of air and pressure losses along the feeding system. As a result of this process real volumetric efficiency of the cylinder and the engine performance as a whole, can not meet the design expectations if all effects were not considered correctly. One component that plays an important role in this process of air supply is the intake manifold (IM), whose physical characteristics such as pressure loss imposed on air and lack of homogeneity of the loss between the runners (air supply unbalanced) are some of the factors that are linked to fuel consume efficiency and engine emissions.

Given that the admission process takes place in a pulse, by opening and closing the intake valves during the engine piston travel down, which introduces rapid variations in pressure and flow to excite the internal volumes of the IM.

Thus, according to Winterbone and Pearson (1999), the pulsating nature of admission is extremely dependent on the rotation of ICE and hence the IM impedance or admittance is a function of frequency of input pulses, where impedance and admittance are volume's acoustic characteristics. Because of these effects is that you can tune to an IM as a function of rotation. In Winterbone and Pearson (1999) also, it is described that the operation of an ICE, after opening the inlet valve and downward movement of the piston during the time of induction of the air / fuel mixture, reduces the pressure in the cylinder and causes a rarefaction wave which travels the IM to its walls, volumes and ducts, which cause attenuation, resonances or reflection effects, similar of the acoustics wave traveling through.

1.1 Dynamic flow

Winterbone and Pearson (1999 and 2000) claim that those pulsed admission processes should be treated as wave phenomena, similar to sound waves that occur in volumes, ducts and passageways into the IMs.

At Fig. 1, 2 and 3 it is possible to see the variation of the pressure in time for an ICE in 1500, 3000 and 6000 rpm respectively, from simulation results, which shown that the variation of engine speed do a influence in the pressure profile.

Consequently, the IM cavity is excited by that pressure variation and the IM volume, shape and passageways resonates according to wave theory of sound, in addition of fluid inertia effects.

M. Cavaglieri, T. Moura and R. Santos
An Experimental Approach For Intake Manifold Tuning For Internal Combustion Engines

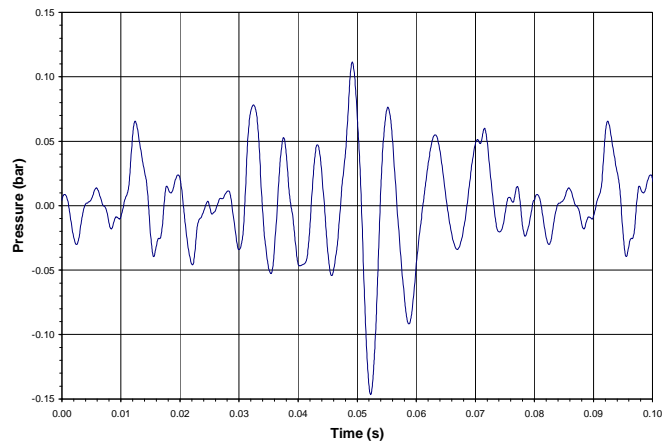


Figure 1. Pressure versus time by one cylinder for ICE at 1500 rpm

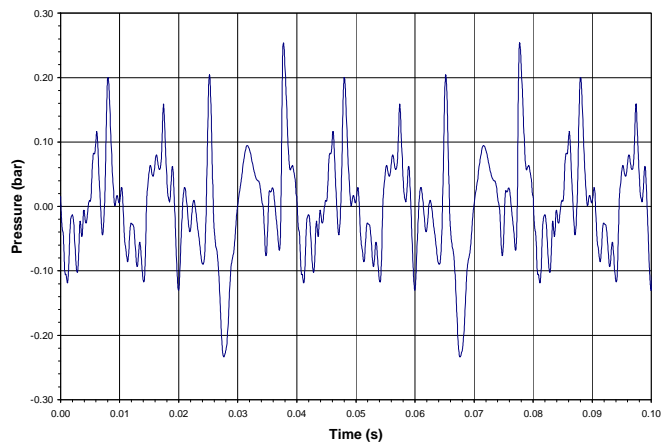


Figure 2. Pressure versus time by one cylinder for ICE at 3000 rpm

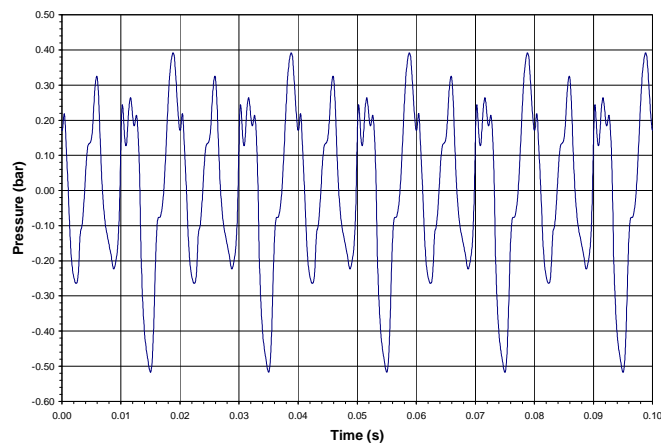


Figure 3. Pressure versus time by one cylinder for ICE at 6000 rpm

There are numerous technologies already implemented by several automakers who sell vehicles with technology that exploits the varying geometry of IMs, aiming to tune it properly for every engine speed or a range of rotation. A simple form is presented by Ford in Thomas, M.A. and Collingwood (1992), where two different arrangements are switched in a specific rotation. See Fig. 4 for an illustration of the concept of varying geometry.

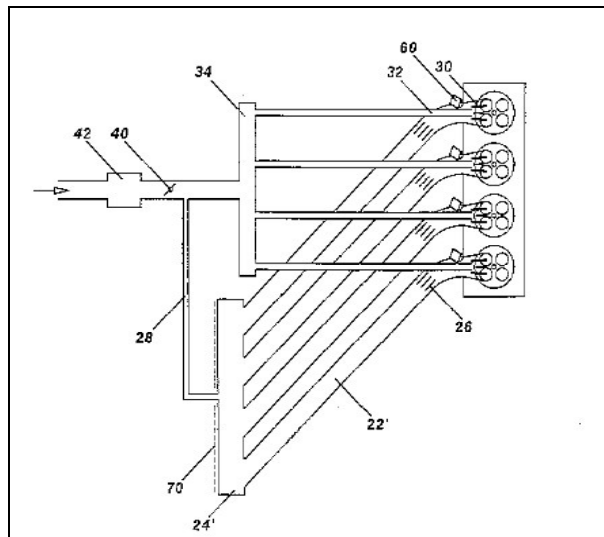


Figure 4. Intake manifold with variable geometry scheme taken from Ford patent, Thomas, M.A. and Collingwood (1992)

In Fig. 4, a simplified interconnection valve (number 28) switches the two sets composed by plenum and tubes with different shapes and sizes, suitable for different ranges of ICE's rotation. In practice, the mechanism works as shown on a Honda's product in Kenji (2011), which shows in detail how it is done switching between channels and redirecting flow in every situation.

Other products are presented by Joo (2009), Mashiko (2006), Stefan (2006) and Pascal (2006), which show other techniques used by Hyundai, Mitsubishi, Volkswagen and Renault respectively, to vary the length of the runners, change volume, combinations of these, and other characteristics of geometry, which can cause the IM tuning discretely or continuously to the MCI's rotation, or rather the need to feed the combustion chamber in each condition and opening duration of the intake valve.

2. FUNDAMENTALS

Considering the cited relation between performance and acoustic parameters, in this paper we will consider just the acoustic cavity properties or its effect in wave transmission.

As shown by Munjal (1987) and Barron (2003) the most appropriate way to quantify the effect that a component like an IM would cause in the propagation of acoustic waves is measuring the acoustic transmission loss (TL), because this parameter characterizes the component independent of the source and the medium where the wave will propagate. As demonstrated by Barron (2003) the TL is given by Eq. (1).

$$TL \equiv 10 \text{Log}_{10} \left(\frac{1}{at} \right) \quad (1)$$

Where at is the acoustic transmission coefficient given by:

$$at \equiv \frac{W_{out}}{W_{in}} = \frac{I_{out}}{I_{in}} = \frac{\left(\frac{p_{out}^2}{Z_{out}} \right)}{\left(\frac{p_{in}^2}{Z_{in}} \right)} \quad (2)$$

Considering that:

- W_{out} outlet power
- W_{in} inlet power
- I_{out} outlet intensity
- I_{in} inlet intensity
- p_{out} outlet wave pressure
- Z_{out} outlet impedance
- p_{in} inlet wave pressure
- Z_{in} inlet impedance.

In this paper, for a convenience, the transmission coefficient at , or their logarithmic representation, will be used as a parameter because it is directly related to what is intended, to maximize the transmission of air through the ICE. The relationship we want to show here is that as higher the coefficient, as better the transmission wave from outside the IM component to the ICE induction valve. Considering that power, intensity or pressure / impedance and all of them are frequency dependent the at coefficient is going to be too. So each IM will have four curves of this coefficient in function of frequency, since these IMs tested here are to 4-cylinder engines.

Experimentally, like a revision done by Tao (2003) the TL can be determined by several methods, among of them are decomposition method, Crooks method and four pole method. As also explained by Tao and Seybert (2003) and Nuñez *et al* (2008) the four poles determination technique is more stable and provides more consistent results with analytical and numerical models and can be accomplished by changing the terminating apparatus called as two load method. This method, shown by Munjal (1987) and a nearest application of this paper work in the Nuñez *et al* (2008) is based on the arrangement where a transfer matrix of the acoustic element can be modeled by four poles, and determined by Eq. (3) like a transfer matrix.

$$\begin{bmatrix} p_i \\ v_i \end{bmatrix} = \begin{bmatrix} A_{ij} & B_{ij} \\ C_{ij} & D_{ij} \end{bmatrix} \begin{bmatrix} p_j \\ v_j \end{bmatrix} \quad (3)$$

Where p_i and p_j are sound pressures at the inlet and outlet, v_i and v_j are the particle velocities at the inlet and the outlet, respectively, shown at Fig. 5, the A_{ij} , B_{ij} , C_{ij} , and D_{ij} are the four-pole parameters. The inlet and outlet points are chosen as close as possible to the pipe ends.

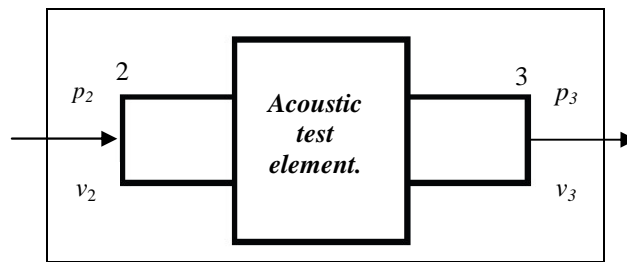


Figure 5. four poles representation

To compute the transfer matrix elements, also called four-pole parameters, we employ Two-load method, like exposed by Tao and Seybert (2003). In this method two different terminations are applied to obtain p_2 , p_3 , v_2 , and v_3 . Configuration *a* has a rigid termination and the Configuration *b* represents the measurements done under anechoic termination.

The expression for the transmission loss using the two-load method, like demonstrated by Munjal (1987) and Gerges (2005) is the Eq. (4).

$$TL = 20 \log_{10} \left\{ \frac{1}{2} \left| A_{23} + \frac{B_{23}}{\rho c} + \rho c \cdot C_{23} + D_{23} \right| \right\} + 10 \log_{10} \left(\frac{S_{in}}{S_{out}} \right) \quad (4)$$

Where, according to Mo (1994) and Gerges (2005), the matrix elements A_{23} , B_{23} , C_{23} and D_{23} are obtained from the four pole matrix and are given by:

$$A_{23} = \frac{\Delta_{34} (H_{32a} H_{34b} - H_{32b} H_{34a}) + D_{34} (H_{32b} - H_{32a})}{\Delta_{34} (H_{34b} - H_{34a})} \quad (5)$$

$$B_{23} = \frac{B_{34} (H_{32a} - H_{32b})}{\Delta_{34} (H_{34b} - H_{34a})} \quad (6)$$

$$C_{23} = \frac{(H_{31a} - A_{12} H_{32a}) (\Delta_{34} H_{34b} - D_{34b}) - (H_{31b} - A_{12} H_{32b}) (\Delta_{34} H_{32a} - D_{34a})}{B_{12} \Delta_{34} (H_{34b} - H_{34a})} \quad (7)$$

$$D_{23} = \frac{B_{34}[(H_{31a} - H_{31b}) + A_{12}(H_{32b} - H_{32a})]}{B_{12}\Delta_{34}(H_{34b} - H_{34a})} \quad (8)$$

In the Eq. (5) to Eq. (8) where Δ are the determinants from matrix, $\Delta_{ij} = A_{ij}D_{ij} - B_{ij}C_{ij}$. The H_{ij} are transfer functions to the a and b different terminations, like explained before and the transfer functions are given by:

$$H_{ij} = \frac{G_{ij}}{S_{ii}} \quad (9)$$

Where G_{ij} is the cross spectrum from microphone i to microphone j , and S_{ii} is the auto spectrum of the microphone i . For the tests here it will be assume no flow, because the measurements are done in IM with no air flow through it in this way, the transfer matrix of four poles has its data elements by:

$$\begin{bmatrix} A_{12} & B_{12} \\ C_{12} & D_{12} \end{bmatrix} = \begin{bmatrix} \cos(kx_{12}) & j \rho \operatorname{sen}(kx_{12}) \\ \frac{j \operatorname{sen}(kx_{12})}{\rho c} & \cos(kx_{12}) \end{bmatrix}, \Delta_{12} = 1 \quad (10)$$

$$\begin{bmatrix} A_{34} & B_{34} \\ C_{34} & D_{34} \end{bmatrix} = \begin{bmatrix} \cos(kx_{34}) & j \rho \operatorname{sen}(kx_{34}) \\ \frac{j \operatorname{sen}(kx_{34})}{\rho c} & \cos(kx_{34}) \end{bmatrix}, \Delta_{34} = 1 \quad (11)$$

The k relation is defined like wave number ($k = \omega/c = 2\pi/\lambda$) where, ω is the angular frequency, c and ρ the sound velocity and the density in the medium respectively and λ the wavelength, the x_{ij} is the distance between microphone i and microphone j .

3. EXPERIMENTAL APPROACH

In Fig. 6 it can be seen the experimental setup used to determine the acoustic transfer coefficient for IM. The outlet tube is connected to one runner at a time and every other runners are capped, so that no sound comes through them. Thus, there is a set of four curves for each IM, one for each runner.

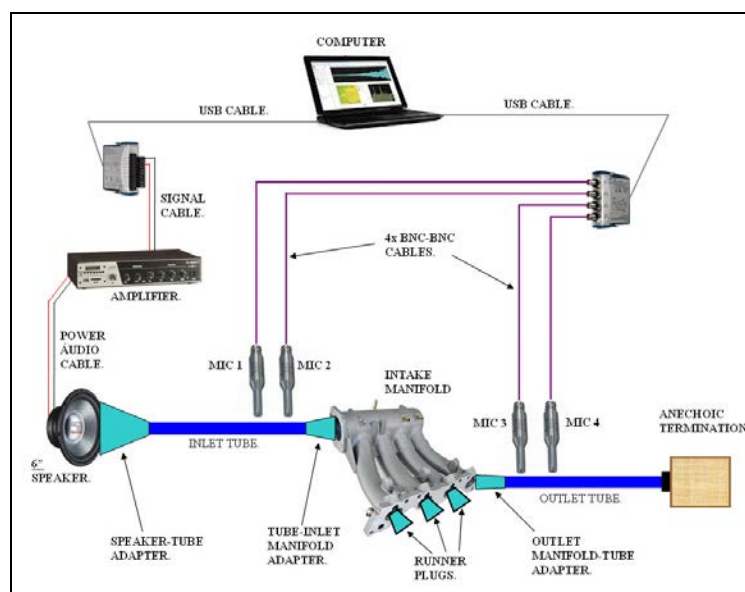


Figure 6. Experimental approach sketch

To perform the acoustic excitation a signal generator installed in computer was used to create a random signal white noise, which is a signal composed by a broad band of frequencies, then conditioned by an audio amplifier that feeds a

speaker type mid-bass. It also used two pairs of microphone 7 mm in diameter, type pre-polarized and pre-amplifier built into the same body. This type of microphone is used in various tests arrangement, commonly for acoustic holography. The inlet and outlet tubes to insert and capture pressure waves are tubes in PVC of 35 mm internal diameter, 700 mm long and 2.5 mm wall thickness.

3.1 System calibration

For calibration and adjustment of the experimental setup it was used a reference volume which can be determined its transmission coefficient analytically.

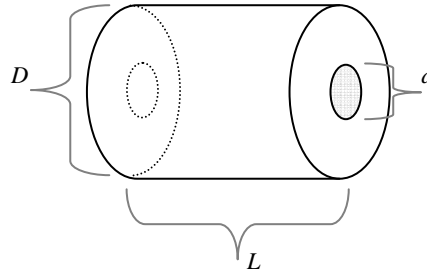


Figure 7. Reference volume for approach calibration

On Fig. 7, D is the diameter of the cylinder volume, d is the diameter of the inlet and outlet and L is the total length of the volume.

As shown in [10] it is possible to calculate the TL element according to Eq. (12).

$$TL = 10 \log_{10} \left\{ \cos^2 \left(\frac{\pi \cdot f}{2 \cdot f_n} \right) + \frac{1}{4} \left(\frac{S_2}{S_1} + \frac{S_1}{S_2} \right)^2 \cdot \sin^2 \left(\frac{\pi \cdot f}{2 \cdot f_n} \right) \right\} \quad (12)$$

Where f is the excitation frequency and the fundamental frequency f_n of the chamber given by Eq. (13).

$$f_n = \frac{c}{4L} \quad (13)$$

Since S_1 and S_2 are the cross-sectional areas of the inlet duct and the expansion chamber successively. And c is the sound velocity in the medium (air at 20 °C and 1 atm). Using Eq. (1) and Eq. (2) it is possible to extract the acoustic transmission coefficient of such analytical reference volume, thereby obtaining the parameter of interest for the case of this work.

The experimental approach, with the calibration volume can be seen on Figure 8.

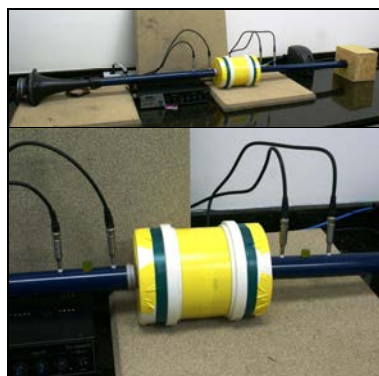


Figure 8. Reference volume on experimental bench (upper: panoramic, bottom: close)

3.2 Calibration analysis

Figure 9 presents a comparison of experimental and analytical *at* curve for volume reference with $d = 35.3$ mm, $D = 151.0$ mm and $L = 203.2$ mm.

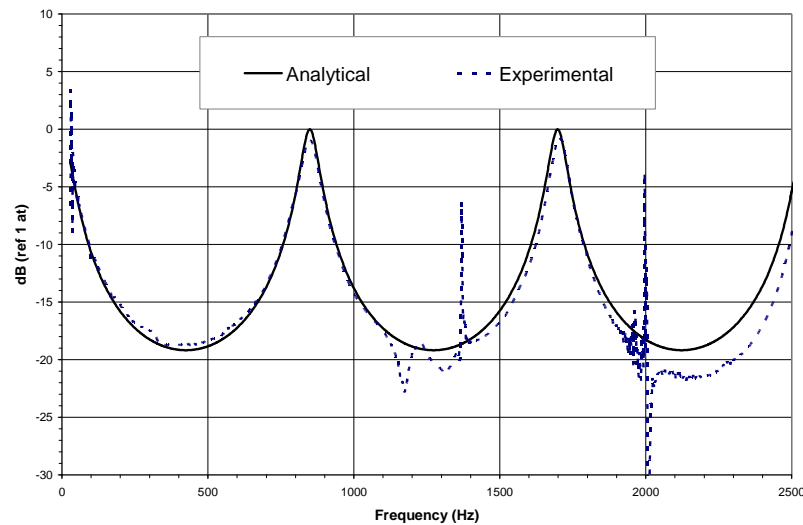


Figure 9. Calibration *at* curve comparison, between experimental and analytical, for reference volume

As seen in Figure 9 the experimental and analytical curves are very similar up to 1100 Hz, where the trial presents a variation that goes up to 1400 Hz. After some tests it was observed that this frequency range is affected by structural mode coupling of the reference volume that was built in plastic tubes which have relatively thin walls, introducing so an inconsistency in measurements.

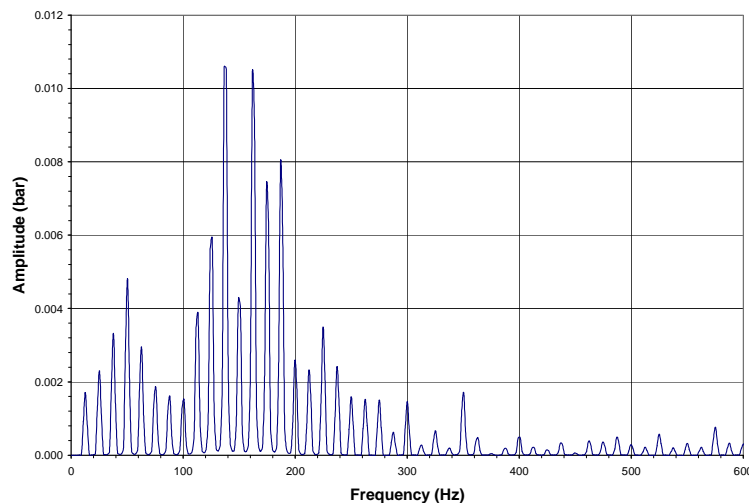
About 1900 Hz was noted that some construction characteristics of couplers and tubing length may had affected, if necessary, it will be investigated to find the sources of these effects and their correlations.

However, in the case of this study, we consider the effects up to 600 Hz, which gives us the possibility to analyze the twelfth (12th) harmonic of the rotation in the worst case, which would be the engine at 6000 rpm. The excitation frequency of an IM cavity is given by the Eq. (14).

$$f_i = i \frac{w}{k \cdot 60} \quad (14)$$

Where w is the engine speed in rpm and i is the order of the harmonic that is intended to find, being fundamental for $i = 1$. The Eq. (14) is drawn from the fact that the IM cavity is excited by the opening of the intake valve, which happens once every two cycles of each cylinder in 4-stroke ICE, so the k value is 2.

Figure 10, 11 and 12 presents the FFT (Fast Fourier Transformation) curve of the pressures presented in Fig. 1, 2 and 3 which shown the relation of the fundamental and n th harmonics for each ICE speed, from numeric model.



M. Cavaglieri, T. Moura and R. Santos
 An Experimental Approach For Intake Manifold Tuning For Internal Combustion Engines

Figure 10. Pressure FFT curve for ICE at 1500 rpm, harmonics 12.5 Hz spaced

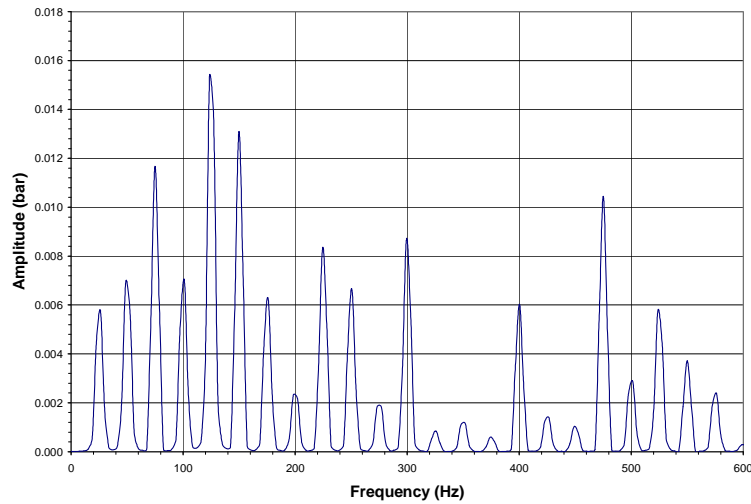


Figure 11. Pressure FFT curve for ICE at 3000 rpm, harmonics 25 Hz spaced

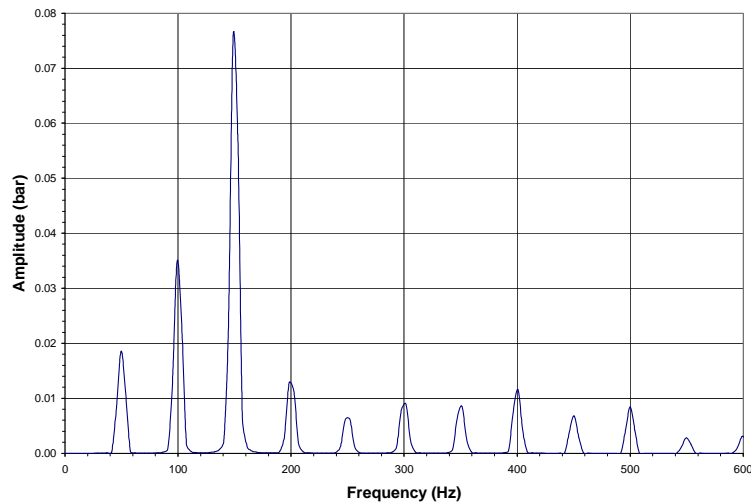


Figure 12. Pressure FFT curve for ICE at 6000 rpm, harmonics 50 Hz spaced

It can be seen that the harmonics are spaced approximately as proposed, confirming the relation of the Eq. (14).

In the graph of Figure 9 can also be observed instability around 30 Hz, this is achieved by the difficulty of generating waves without significant distortion and amplitude in order to have a good signal to noise ratio below 30 Hz. These effects are caused by deficiency of the source used here, even though a speaker covering a wide dynamic range and good quality.

4. RESULTS

Checking Figure 13, it is possible to see a 3D view of the IM which is going to be studied here that in turn it finds applications in two models of engines, in an engine capacity 1.0 and 1.4 liters.

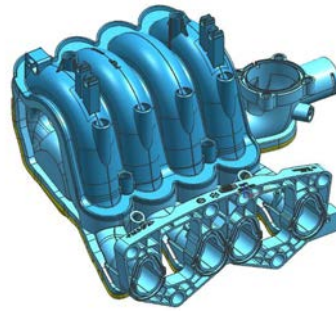


Figure 13. 3D view of the IM studied

In Figure 14 and Figure 15 it is possible to find the torque profile for two IMs installed in both ICEs, where IM - # 02 is an evolution of IM - # 01, which not only the acoustic characteristic studied here is improved, as well as aspects like continuous flow, as presented by Cavaglieri, Moura and Santos (2009). In this way, were measured the torque curve of IMs installed on both engines, in order to verify the benefit brought in two applications.

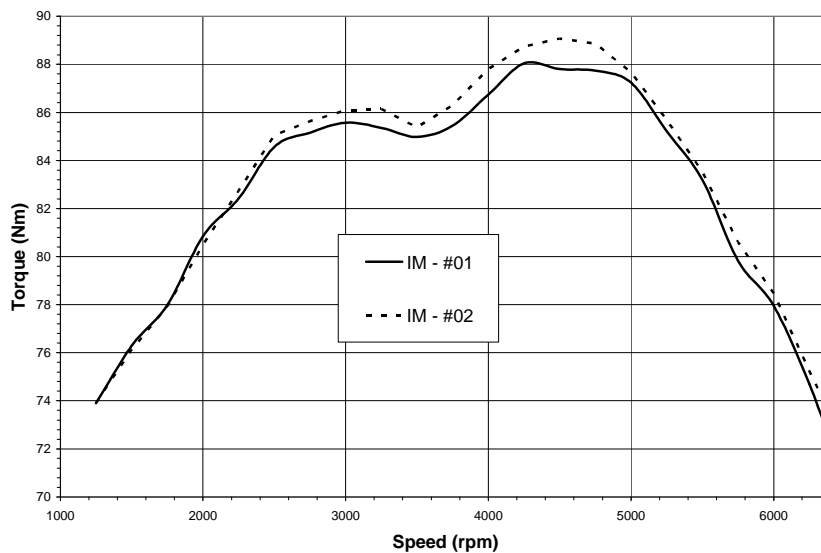


Figure 14. 1.0 liter ICE torque profile

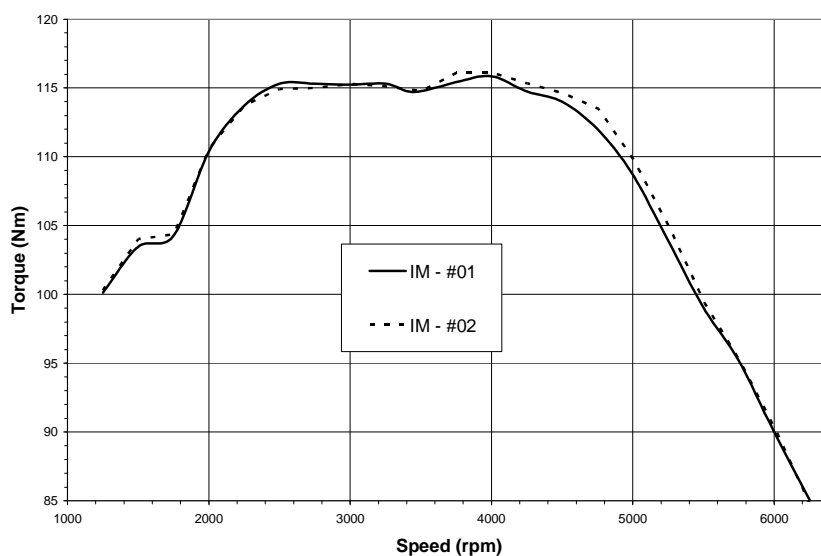


Figure 15. 1.4 liter ICE torque profile

In Figure 16 are shown transmission coefficient curves, raised from the experimental procedure for both IMs.

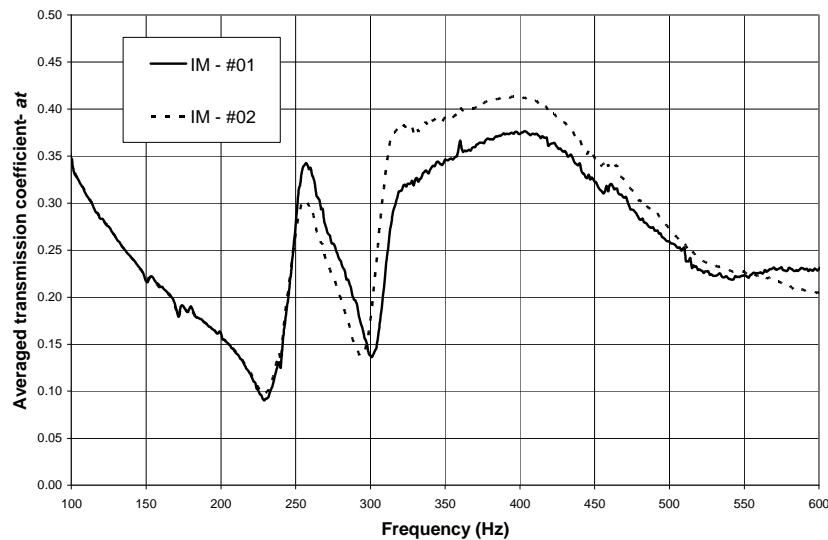


Figure 16. Averaged coefficient \overline{at} comparison for IM - #01 and IM - #02

The comparison is the averaged \overline{at} coefficient, because as stated earlier, that are extracted a curve for each runner and the average coefficient calculated for the IM as a whole which has a complex number and hence the average is obtained by Eq. (15).

$$\overline{at} = \frac{\sum_{i=1}^n \sqrt{\text{Re}(at_i)^2 + \text{Im}(at_i)^2}}{n} \quad (15)$$

Where n is the number of runners of the IM which has, for this case, $n = 4$. The $\text{Re}(at)$ is the real part of at and $\text{Im}(at)$ its imaginary part.

5. CONCLUSION

As shown in the Calibration section, the experimental apparatus had to be stable and reproduces the analytical model in a frequency range wide enough for studies intended. In order to achieve a quality curve is essential to have two very different endings, as mentioned in item analysis of calibration.

The ends must be as much different as possible (rigid versus anechoic) in the frequency range of interest. A method for characterizing impedance termination is shown by Seybert and Ross (1976) and it can be applied the same experimental apparatus described here, with a simpler arrangement.

Tests for IMs and their ICE torque curves, showed that the geometry change brought an improvement on torque profile and also effectively increased the "at" parameter, indicating that the dynamic behavior of admission through an IM has some correlation with wave transfer. The derivation of this relationship will be the subject of future studies that will complement the theory started here.

6. ACKNOWLEDGEMENTS

We would like to thank all friends of the company who contributed to this study be possible, especially to Engineer Luiz Fernando Windlin by continuous encouragement, that gives such projects in all directions, spreading the scientific spirit in the workplace.

We also thank the staff of LMS South America in the people of Eng. Henrique Abrão and Eng. Charles Croufer, who put their equipment and software at our disposal for the experimental measurements were carried out in a practical and easy to obtain.

7. REFERENCES

22nd International Congress of Mechanical Engineering (COBEM 2013)
November 3-7, 2013, Ribeirão Preto, SP, Brazil

- Cavaglieri, M. R., Moura T. M. and Santos, R. G., 2009. "Correlation between Numeric Simulation and Experimental Results on Intake Manifold Development," SAE Technical Paper 2009-36-0274.
- Barron, R. F., 2003. "Industrial Noise Control and Acoustics," 1st Edition. ed. Nova Yorque: Marcel Dekker Inc.
- Gerges, S. N. Y. and Jodan, R., 2005. "Muffler Modeling by Transfer Matrix Method and Experimental Verification
- Joo, J. Y., 2009. "Variable Intake Manifold," Patent KR20090065380, Hyundai Motor Company.
- Kenji, T., 2011. "Engine Intake Control Device," Patent JP2011064139, Honda Motor.
- Masahiko, K., 2006. "Variable Intake System," Patent JP08338252, Mitsubishi Motors Corp.
- Munjaj, M. L., 1987. "Acoustics of Ducts and Mufflers". John Wiley & Sons.
- Nuñez, I. J. C., De Marqui, A. L. L., Cavaglieri, M. R., Arruda, J. R. F., 2008. "Investigating the Transmission Loss of Compressor Suction Mufflers Applying Experimental and Numerical Methods," *International Compressor Engineering Conference*, Purdue, Indiana, USA on July 14-17 of 2008, 8p.
- Pascal, C., "Variable intake system for combustion engines and pipe element for such a device," Patent EP1083310, Renault, 2006.
- Seybert, A. F., Ross, D. F., "Experimental determination of acoustic properties using a two-microphone random-excitation technique," Technical Paper University of Kentucky, 1976.
- Stefan, L., 2006. "Suction System for Supplying an Internal Combustion Engine With Combustion Air," Patent EP1049859, Volkswagen AG.
- Tao, Z., Seybert, F., 2003. "A Review of Current Techniques for Measuring Muffler Transmission Loss, Proc. SAE Noise and Vibration Conference, Michigan," USA.
- Thomas, M.A. and Collingwood, T.H., 1992. "Tuned Engine Manifold," Patent US5441023, Ford Motor Co.
- Winterbone, D. E. and Pearson, R. J., 1999. "Design Techniques for Engine Manifolds," SAE Publication.
- Winterbone, D. E. and Pearson, R. J., 2000. "Theory of Engine Manifold Design – Wave action methods for IC engines," SAE Publication.

8. RESPONSIBILITY NOTICE

The authors are the only responsible for the printed material included in this paper.